Separation Science and Technology
Publication details, including instructions for authors and subscription information:
http://www.informaworld.com/smpp/title~content=t713708471

Immobilization of Cyphos Ionic Liquids in Alginate Capsules for Cd(II) Sorption

E. Guibal[a]; A. Figuerola Piñol[ab]; M. Ruiz[b]; T. Vincent[a]; C. Jouannin[a]; A. M. Sastre[c]
[a] Ecole des Mines d'Alès (France), Laboratoire Génie de l'Environnement Industriel, Ales cedex, France [b] Department of Chemical Engineering, Universitat Politècnica de Catalunya, E.U.P.V.G., La Geltru, Spain [c] Department of Chemical Engineering, Universitat Politècnica de Catalunya, E.T.S.E.I.B., Barcelona, Spain

Online publication date: 30 August 2010

To cite this Article Guibal, E. , Piñol, A. Figuerola , Ruiz, M. , Vincent, T. , Jouannin, C. and Sastre, A. M.(2010) 'Immobilization of Cyphos Ionic Liquids in Alginate Capsules for Cd(II) Sorption', Separation Science and Technology, 45: 12, 1935 — 1949
To link to this Article: DOI: 10.1080/01496395.2010.493113
URL: http://dx.doi.org/10.1080/01496395.2010.493113

Separation Science and Technology, 45: 1935–1949, 2010

ISSN: 0149-6395 print/1520-5754 online
DOI: 10.1080/01496395.2010.493113

Taylor & Francis
Taylor & Francis Group

Immobilization of Cyphos Ionic Liquids in Alginate Capsules for Cd(II) Sorption

E. Guibal,[1] A. Figuerola Piñol,[1,2] M. Ruiz,[2] T. Vincent,[1] C. Jouannin,[1] and A. M. Sastre[3]

[1]*Ecole des Mines d'Alès (France), Laboratoire Génie de l'Environnement Industriel, Ales cedex, France*
[2]*Department of Chemical Engineering, Universitat Politècnica de Catalunya, E.U.P.V.G., La Geltru, Spain*
[3]*Department of Chemical Engineering, Universitat Politècnica de Catalunya, E.T.S.E.I.B., Barcelona, Spain*

Four phosphonium ionic liquids (Cyphos IL-101, IL-105, IL-109, and IL-111) have been immobilized in composite biopolymer capsules (alginate/gelatin). The resins were tested for Cd(II) sorption in HCl solutions. Cyphos IL-111 being solid at room temperature, the phase change contributes to the formation of large vesicles in the resin particle. Sorption isotherms were not affected by the anionic counterpart (chloride, dicyanamide, or tetrafluoroborate), except with bistriflamide (Cd(II) was not sorbed). HCl concentration (0.1–4.6 M) did not influence the Cd(II) uptake (60 mg Cd g^{-1}). Kinetic profiles were modeled using the intraparticle diffusion equation. Highly porous foams have been developed as an alternative to resin beads in order to improve diffusion characteristics.

Keywords cadmium; desorption; diffusion; immobilization; isotherms; sorption; tetraalkylphosphonium ionic liquids

INTRODUCTION

Regulations on wastewater treatment and discharge to the environment have drawn for the last decades great attention on the development of alternative processes for metal recovery from secondary sources. The treatment of spent batteries is an emblematic example of these new trends (1–4). The presence of hazardous metals such as cadmium, associated with other metals (5,6), requires the combination of different treatment sequences for the elimination of the metal and its separation from other base metals. The obligation to treat waste materials (for limiting environmental impact and for product recycling and valorization) before landfill discharge is another driving force for the development of new processes. Hydrometallurgy remains one of the most appropriate strategies for the recovery of metals from solid wastes (7). After solid to liquid transfer (acidic leaching in most cases), different processes can be used for metal separation and valorization, depending on the concentration range, the value of target metals, and the flows rates (8,9): precipitation, liquid-liquid extraction (10,13), sorption on resins (14–17). Solvent/Extractant impregnated resins (SIRs) combine the benefits of resins and solvent extraction systems (i.e., the high efficiency of solvent extraction and the confinement properties of resins). SIRs have been used for cadmium recovery from acidic solutions (18–21). Ionic liquids (IL) offer promising perspectives for the replacement of the solvent (22), or extractant (23–25) in the liquid/liquid extraction process.

Tetraalkylphosphonium-based ILs were tested for metal extraction (26,27) and the recovery of organic acids (28,29). Immobilizing the ionic liquids on solid supports opens the route to a new class of SIRs (30–34). Recently, biopolymers have been used for the immobilization of conventional extractants (35–40), and ionic liquids (41–45) for metal recovery. Chitosan and alginate are examples of renewable resources that were used for the "encapsulation" of extractants and ionic liquids taking advantage of their easy conditioning and high affinity for metal binding (46–49). The combination of alginate and gelatin polymers allowed immobilizing Cyphos IL-101 (tetraalkylphosphonium ionic liquid) for the synthesis of resins for Pt(IV) (42), Pd(II) (41), Au(III) (44), Bi(III) (45), and Hg(II) (43) recovery. It appeared interesting to check the influence of the counteranion of the IL on the sorption properties of the resins. This work focuses on the study of Cd(II) recovery from HCl solutions with resins impregnated with different tetraalkylphonium-based ILs (substituted with different counteranions, i.e., chloride, dicyanamide, bistriflamide and tetrafluoroborate, Table 1).

Received 4 February 2010; accepted 16 March 2010.
Address correspondence to Eric Guibal, Ecole des Mines d'Alès, Laboratoire Génie de l'Environnement Industriel, Ales cedex, F-30319, France. Tel.: +33(0)466782734; Fax: +33(0) 466782701. E-mail: Eric.Guibal@mines-ales.fr

TABLE 1
Characteristics of ionic liquids and IL-immobilized alginate capsules

Nomenclature	MW	Anion	Capsule Diameter	IL content	W.C.
trihexyl(tetradecyl)-phosphonium chloride Cyphos IL-101	519.42	Cl^-	0.49 ± 0.03	0.95	88
trihexyl(tetradecyl)-phosphonium dicyanamide Cyphos IL-105	550.02	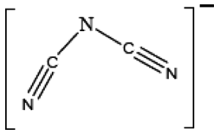	0.45 ± 0.09	0.93	89
trihexyl(tetradecyl)-phosphonium bistriflamide Cyphos IL-109	764.14	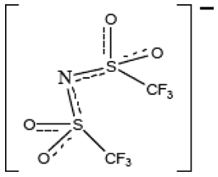	0.53 ± 0.06	0.80	87
trihexyl(tetradecyl)-phosphonium tetrafluoroborate Cyphos IL-111	570.78	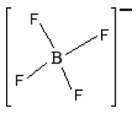	0.31 ± 0.02	0.88	89

MW: Molecular weight (g/mol); Diam.: diameter (μm, in the dry state); IL content (mmol g^{-1}, dry weight); W.C.: water content (% on wet weight).

The first part of the work compares the sorption properties of the different ILs immobilized in biopolymer capsules with attention paid to:

(a) the influence of HCl concentration,
(b) sorption isotherms, and
(c) uptake kinetics (under selected experimental conditions).

The investigation of uptake kinetics is pursued on Cyphos IL-101 with a focus on the effects of agitation speed, metal concentration, and sorbent dosage. In the third part, desorption and sorbent recycling are carried out.

MATERIAL AND METHODS

Materials

The ILs were supplied by Cytec (Canada): Cyphos® IL-101, IL-105, IL-109, IL-111 (see Table 1 for chemical structure and molecular weight). All of them are liquid at room temperature, except IL-111, which is liquid only above 35–37°C. Alginate was supplied by Acros Organics (Switzerland) and gelatin by VWR Prolabo (France). Other reagents (metal salts, NaCl, $NaNO_3$, mineral acids) were supplied, as reagent grade products, by Fluka AG (Switzerland).

Ionic Liquid Immobilization

The synthesis of the Cyphos-impregnated resins was performed in 2 steps:

(a) A given amount of IL (i.e., 24 mmol) (corresponding to a variable mass of IL; i.e., 12.5, 13.3, 18.4 and 13.8 g for IL-101, IL-105, IL-109, and IL-111, respectively), previously mixed with 2.5 mL of a 10 M NaOH solution was mixed with 25 g of a 20% (w/w) aqueous solution of gelatin. This solution was added to a solution of sodium alginate (2%, w/w) for a total volume of 500 mL. The mixture was prepared under ultrasonic treatment to homogeneously distribute the IL in the composite biopolymer solution. A slightly viscous white emulsion was obtained.
(b) The stable emulsion was then dropped through a thin nozzle (internal diameter 0.6 mm) into an ionotropic gelling solution ($CaCl_2$, 6% in water, w/w).

Note: The gelatin was heated to make it liquid and miscible with the IL and with alginate. Gelatin served as a stabilizer of the emulsion. This was sufficient for making liquid the IL-111 sample (which is solid below 37°C). However, it was necessary using a double-envelope reactor (with warm water circulation) for maintaining an appropriate temperature during the extrusion procedure (to prevent IL-111 solidification before ionotropic gelation). The alkaline gelatin solution contributes to make the hydrophobic IL compatible with alginate aqueous solution.

The beads were maintained in the coagulation bath overnight before being rinsed with 0.1 M HCl solution. They were stored in 0.1 M HCl, in order to prevent possible degradation of the composite biopolymer matrix. Based on poor alginate stability in alkaline and neutral solutions, the material can only be used in acidic conditions such as those

produced in the acidic leaching of waste material or secondary metal sources.

Resin Characterization

The water content of the resin was determined by weight loss after drying at room temperature for 24 hours. The size of particles was determined by measurement of the beads diameter on scanning electron microphotographs. The resin particles were also visualized through a rear projector (expanding the size) for the measurement and the statistical analysis of the size of resin particles as a complementary determination to microscope observation.

The ionic liquid content was determined by phosphorus analysis using ICP-AES (Inductively Coupled Plasma Atomic Emission Spectrometry, JY 2000, Jobin-Yvon, Longjumeau, France) after chemical degradation of the polymer matrix. A known amount of resin (i.e., 60–100 mg) was mixed with 2 mL of sulfuric acid and heated till complete mineralization occurred (destruction of polymer capsule). After cooling, 1 mL of hydrogen peroxide was added drop by drop. The mixture was heated till the bubbles disappeared and discoloration was complete. After cooling and volumetric adjustment, the P content was measured to evaluate the molar IL concentration in the resin. Table 1 gives the main characteristics of the resins prepared by this procedure (particle size, IL-content, and water content).

Scanning electron microscopy (SEM) and SEM-EDAX (SEM coupled with energy dispersive X-ray analysis) were performed using an Environmental Scanning Electron Microscopy (ESEM) Quanta FEG 200, equipped with an OXFORD Inca 350 Energy Dispersive X-ray microanalysis (EDX) system. The system can be used to acquire qualitative or quantitative spot analyses and qualitative and semi-quantitative X-ray elemental maps and line scans. For cross-section analysis, the resin particles were frozen in liquid nitrogen prior to a mechanical breaking in order to obtain observable cross-sections. Though the cross-section is less regular than with a thin-slice cutter, this procedure prevents the section to be contaminated by element dispersion.

Sorption Studies

For the evaluation of equilibrium performance a volume of acid solution (i.e., 80 mL in most cases) containing the appropriate concentration of Cd was mixed with a known amount of resin (i.e., 50 mg). The slurry was agitated for 72 hours to be sure to reach equilibrium. Actually, the kinetic study showed that a shorter contact time could be sufficient. This long equilibrium time was selected for insuring that all accessible and available reactive groups could be saturated. The residual concentration of Cd was measured by ICP-AES analysis after filtration. The sorption capacity (q, mg Cd g^{-1} or mmol Cd g^{-1}) was determined by the mass balance equation: $q = V(C_0\text{-}C_{eq})/m$, where C_0 and C_{eq} are the initial and equilibrium concentrations (mg Cd L^{-1} or mmol Cd L^{-1}) of Cd, respectively; V is the volume of solution (L) and m the mass of resin (g). Sorption isotherms were obtained by mixing fixed amounts of resin (i.e., 50 mg) with fixed volumes (i.e., 80 mL) of HCl solutions (at concentrations: 0.1 M, 1 M), containing Cd(II) concentrations in the range 50–200 mg Cd L^{-1}. At equilibrium, the residual concentration was measured to calculate the sorption capacity.

Uptake kinetics were investigated by adding, under agitation, a known amount of resin (i.e., 125 mg, 250 mg, 400 mg or 650 mg of resins, dry weight) to 1 L of Cd (C_0: 25–100 mg Cd L^{-1}) solutions prepared in 1 M HCl solutions. A low sorbent dosage was selected in order to detect the contribution of intraparticle diffusion resistance. Samples were collected, filtered, and analyzed at fixed times.

Desorption was performed by mixing the loaded sorbent (50 mg of sorbent loaded in a 80 mL solution of cadmium at the concentration of 50 mg Cd L^{-1}) with a known volume of eluent (nitric acid, sulfuric acid, and hydrochloric acid, at concentrations 0.1 and 0.5 M) for fixed contact time (i.e., 2 h). The amount of cadmium released was used for calculating the Cd desorption efficiency. For the study of resin recycling, a rinsing step was carried out (using a 0.1 M HCl solution) before using the resin for the next adsorption step. The amount of Cd bound to the resin and subsequently desorbed was obtained by the mass balance equation for the sorption and elution steps, respectively. A comparison of these values enabled the desorption yield (%) to be calculated.

Modeling of Sorption Isotherms and Uptake Kinetics

The sorption isotherms were modeled using the Langmuir equation:

$$q = \frac{q_m b C}{1 + bC} \tag{1}$$

where q_m is the maximum sorption capacity or sorption capacity at saturation of the monolayer (mg g^{-1}), and b is the Langmuir constant (affinity coefficient of the sorbent for the solute). Mathematica™ software was used for the determination of q_m and b parameters using a non-linear regression analysis (limiting the statistical bias that can be introduced by the linearization of the Langmuir equation, $q/C_{eq} = f(C_{eq})$), and for plotting simulated curves on sorption isotherms.

Several steps may control the sorption kinetics:

(a) mass transfer of the solute through the external film and in the porous network (surface and homogeneous diffusion);
(b) reaction rate.

In most cases, binding is controlled by diffusion mechanisms rather than the reaction rate. Since the pioneering work on dynamics of ion exchange processes by Streat (50) and Helfferich (51), Juang and Ju (52) discussed a series of simplified modeling systems derived from the homogeneous diffusion model (HDM) and the shrinking core model (SCM). The HDM involves counterdiffusion of exchangeable species in quasi-homogeneous media, with a contribution from film diffusion (HDM-FD) and/or particle diffusion (HDM-PD). Solute molecules and exchangeable species (immobilized on the resin) follow a similar diffusion mechanism (but in the opposite direction). In the case of the SCM, a sharp virtual boundary exists between the reacted shell of the particle and the unreacted core, and this boundary moves towards the center of the particle (53,54). This model was developed with different systems depending on the controlling step: film diffusion (SCM-FD), particle diffusion (SCM-PD), and the chemical reaction rate (SCM-CR) (52). The equations describing these systems are reported below.

Homogeneous Diffusion Model

$$\text{Film Diffusion:}\quad F_1(X) = -\ln(1-X) = f(t) \tag{2}$$

$$\text{Particle Diffusion:}\quad F_2(X) = -\ln(1-X^2) = f(t) \tag{3}$$

Shrinking Core Model

$$\text{Film Diffusion:}\quad G_1(X) = X = g\left(\int_0^t C(t)dt\right) \tag{4}$$

Particle Diffusion:

$$G_2(X) = 3 - 3(1-X)^{2/3} - 2X = g\left(\int_0^t C(t)dt\right) \tag{5}$$

Chemical Reaction Rate:

$$G_3(X) = 1 - (1-X)^{1/3} = g\left(\int_0^t C(t)dt\right) \tag{6}$$

Where X is the fractional approach to equilibrium (i.e., $q(t)/q_{eq}$), the amount of metal adsorbed at time t divided by the amount of metal adsorbed at equilibrium. Plotting F_i and G_i functions versus time and the integral term (respectively) determined the most appropriate mechanism for describing the controlling step. The simulated curves showing a straight line (best correlation) identify the controlling mechanism. The systems involving the control of kinetics by the resistance to intraparticle diffusion systematically fitted better experimental data than those controlled by film diffusion or the chemical rate (not shown).

The intraparticle diffusion coefficient (D_e, effective diffusivity, $m^2\,min^{-1}$) was determined using Crank's equation, assuming the solid to be initially free of metal, and the kinetics to be controlled by intraparticle diffusion resistance:

$$\frac{q(t)}{q_{eq}} = 1 - \sum_{n=1}^{\infty} \frac{6\alpha(\alpha+1)\exp\left(\frac{-D_e q_n^2 t}{r^2}\right)}{9 + 9\alpha + q_n^2\alpha^2} \tag{7}$$

$q(t)$ and q_{eq} are the concentrations of the metal in the resin at time t and at equilibrium, respectively.

And q_n non-zero roots of the equation:

$$\tan q_n = \frac{3q_n}{3 + \alpha q_n^2} \tag{8}$$

with

$$\frac{q_{eq}}{VC_o} = \frac{1}{1+\alpha} \tag{9}$$

The Mathematica™ software was used for the determination of the intraparticle diffusion coefficient, D_e, and for the simulation of experimental data (represented by the continuous line on the figures).

RESULTS AND DISCUSSION

Resin Characterization

Table 1 summarizes some of the macroscopic properties of the resins (i.e., particle size, IL and water content). All the resins were characterized by similar water content close to 89% (on the wet state). The immobilization procedure requires using dilute solutions to prepare spherical resin particles. With higher concentrations the extrusion of the very viscous solution does not make possible obtaining spherical resins. This high water content requires the resin to be dried after synthesis to reach appreciable volumetric density of reative sites. Additionally, this high water content may induce the mechanical instability of the hydrogel. However, drying causes significant reduction of the mass transfer performance (43). For maintaining mechanical stability and making easy reproducing experimental conditions all the experiments were performed with dried resins.

More significant differences were observed considering the IL content of these resins. The counteranion influenced the amount of IL immobilized. Though the same amount of IL was initially introduced in the reactive media, the amount of ILs immobilized in the capsules followed the sequence: Cyphos IL-101 > IL-105 ≫ IL-111 ≫ IL-109. These differences are related to the chemical properties of the compounds (hydrophobicity) and to their physical properties. Cyphos IL-111 is solid at room temperature (contrary to other ILs). Despite this physical difference the amount of Cyphos IL-111 immobilized in the capsules

FIG. 1. SEM photograph of IL-immobilized resins (cross-section view).

is consistent with those found with other Cyphos ILs. The reasons for this lack of stability were not clearly established. Previous investigations, using the same encapsulation process (with conventional extractants), showed that the possibility to use this immobilization process was controlled by the acidity of the extractant. Depending on the acid-base properties of the extractant the emulsion was not stable enough to make possible the encapsulation. The physical state of the IL had a more significant impact on the size of resin particles: while Cyphos IL-101, IL-105, and IL-109 (all liquid at room temperature) resins have a diameter close to 0.49 mm, in the case of Cyphos IL-111 a much greater variation of resin particles was observed (close to 0.31 mm, in the dry state). The synthesis procedure (gelatin melting) was sufficient for maintaining Cyphos IL-111 liquid in the first phase of the process. During the distribution of the viscous solution into the ionotropic gelation medium, the temperature change caused the in-situ solidification of the IL in the biopolymer matrix, resulting in a volume restriction of the resin particles. Figure 1 shows the SEM photographs of a cross-section of the resin particles for Cyphos IL-101, IL-105, and IL-111. For Cyphos IL-101 and IL-105 particles the internal porous network was characterized by a homogeneous distribution of very small holes (vesicles with diameters of a few micrometers). Much larger vesicles were observed for Cyphos IL-111 based resins (a few dozens of micrometers). This difference is probably due to the

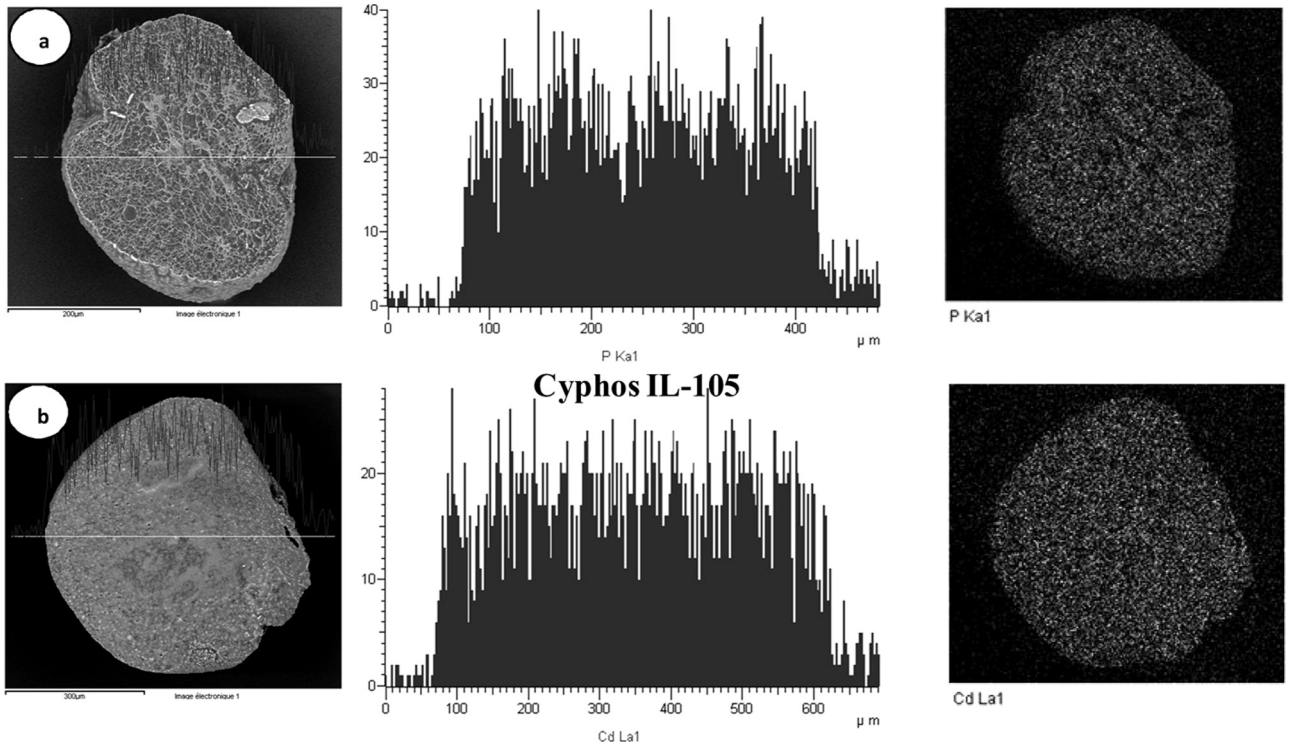

FIG. 2. SEM and SEM-EDAX analysis of a cross-section of Cyphos IL-105-immobilized resin before (a – bar: 200 µm), and after (b – bar: 300 µm) Cd(II) sorption (left: SEM view; center: distribution of P (resin) and Cd (resin after metal sorption) elements through the cross-section; right: cartography of P and Cd elements).

synthesis procedure and the solidification of Cyphos IL-111 during the ionotropic gelation. Figure 2 shows the SEM-EDAX analysis of a cross-section of Cyphos IL-105 resin before and after Cd(II) sorption. The distribution of the P element along the section (and on element cartography) of the resin (prior to metal sorption) shows that the IL is homogeneously distributed in the whole mass of the particle. At sorbent saturation, Cd(II) was also homogeneously distributed in the particle. All the reactive groups remained accessible for metal binding. This analysis is completed by the observation of cross-sections of Cyphos IL-111 resins (before and after metal uptake). The cartography of elements shows the dispersion of the P element in the whole mass of the resin (Fig. 3). However, the distribution of O element (absent from the IL but present in the encapsulating material) serves as a marker of the immobilization matrix. The distribution map for Cd is correlated with the presence of the P element (contrary to the O element). This observation means that Cd(II) was only bound to IL and that the immobilization matrix did not significantly contribute to metal sorption. Despite the affinity of the alginate to divalent cations, under the experimental conditions selected with IL-encapsulated material (i.e., 1 M HCl solutions) the carboxylic acid groups of the biopolymer cannot bind Cd(II). This figure also shows a significant change in the morphology of the resin particle after cadmium binding: while on the as-produced resin (before metal sorption) the porous network was perfectly marked, after metal extraction colloid-like structures formed in the vesicles network. This could be probably related to a mechanism involved in the metal recovery of Pd(II) by reactive precipitation (55): Cyanex 301-biopolymer emulsion (similar composition) was used for the recovery of Pd(II) from HCl solutions. The metal reacted with the organophosphorous extractant simultaneously to the reaction of alginate with HCl (ionotropic gelation) to form flocs.

Influence of HCl Concentration

The immobilizing material is only stable in acidic solutions. In alkaline or neutral media the exchange of calcium or divalent cations with sodium (or potassium) results in the dissolving of the biopolymer and the loss of mechanical structure of the resins. For this reason, the experiments were performed in HCl solutions with concentrations ranging between 0.1 and 5 M. Figure 4 shows that the concentration of the acid did not significantly change Cd(II) sorption on Cyphos IL-101, IL-105, and IL-111 based materials, while for Cyphos IL-109 based resin Cd(II) was absolutely not adsorbed, regardless of HCl concentration. The suspected mechanism consists in the ion exchange/electrostatic attraction mechanism between cationic tetraalkyl phosphonium groups of the ILs and anionic cadmium species ($CdCl_3^-$ or $CdCl_4^{2-}$). The percentage of chloroanionic Cd(II) species strongly varied with HCl concentration (20); from 6% in 0.1 M HCl solution

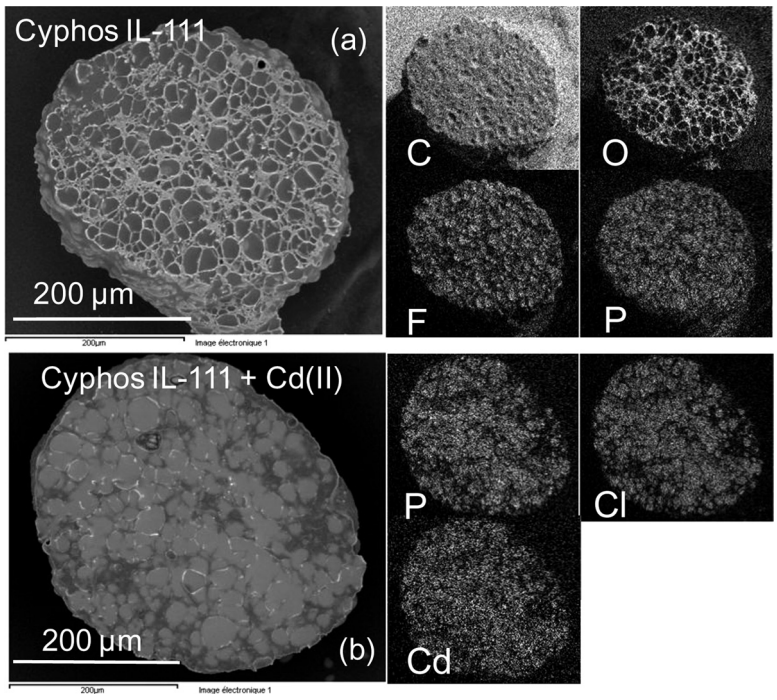

FIG. 3. Cyphos IL-111-immobilized resin before (a) and after (b) Cd(II) sorption – Cross-section view and cartography of C, O, F, P, Cl, and Cd elements (SEM-EDAX analysis).

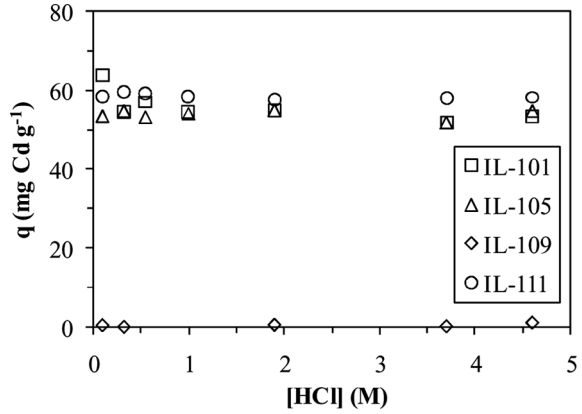

FIG. 4. Influence of HCl concentration on Cd(II) sorption using Cyphos IL-101, IL-105, IL-109 and IL-111 – impregnated resins (C_0: 100 mg L^{-1}; m/V: 625 mg L^{-1}).

to 80% in 4 M HCl solutions. In the case of Cyphos IL-109 the negligible sorption was probably related to the limited capacity of bistriflamide counteranion to be exchanged (at least under selected experimental conditions). This weak efficiency of Cyphos IL-109 is consistent with previous results from Regel-Rosocka (27) who showed that this IL was much less efficient for Zn(II) extraction (in solvent extraction systems) than Cyphos IL-101. The poor efficiency of Cyphos IL-109 was correlated to the higher hydrophobicity of the extractant (related to the imide groups) compared to Cyphos IL-101 that makes difficult the transfer of Zn(II) from the aqueous phase to the organic phase. Cyphos IL-109 resin was not used for further experiments. Under selected experimental conditions, the sorption capacity remained in the range 54–59 mg Cd g^{-1}, for the three resins (with Cyphos IL-101, IL-105 and IL-111), regardless of HCl concentration. The differences imputed to HCl concentration and IL type did not exceed 7%; the three resins appear equivalent regarding Cd(II) sorption in HCl solutions. Despite the effect of HCl concentration on Cd(II) speciation, this parameter has a limited impact. The sorption of Cd(II) occurs through the binding of $CdCl_4^{2-}$ ions (even if they are not predominant). Their binding causes the displacement of the speciation equilibrium toward the formation of chloro-anionic species. The weak effect of HCl concentration contrasts with results previously obtained with, for example, Cyanex 921 immobilized on Amberlite XAD-7 (19). The distribution coefficient (metal concentration in the solid divided by metal concentration in the solution, at equilibrium) increased at low HCl concentration and tended to drastically decrease when HCl concentration exceeded 5 M. In this case the efficiency of sorption depended on the speciation of Cd(II). The efficiency increased with increasing HCl concentration, before decreasing due to a possible change in the predominant metal species. In the case of Zn(II) sorption using Amberlite XAD-7 impregnated with Cyphos IL-101, Gallardo et al. (56) reported the change in the species extracted in function of HCl concentration:

$ZnCl^+$ (with simultaneous binding of Cl^- to form $ZnCl_4^{2-}$ adsorbable species) at low HCl concentration,
$ZnCl_3^-$ (with Cl^- exchange) at intermediary HCl concentration (3–6 M), and $ZnCl_4^{2-}$ (with 2 Cl^- exchange) at high HCl concentration (above 6 M).

Regardless of experimental conditions the extracted species is $(L^+)_2ZnCl_4^{2-}$. In the present case the variation of the distribution coefficient was negligible (not shown). This result is consistent with previous studies on Bi(III) (45), Au(III) (44) or Pt(IV) (42) sorption using comparable systems. With Hg(II) (43), and Pd(II) (41) the sorption efficiency decreased with increasing HCl concentration (though remaining appreciable even at acid concentrations as high as 4–5 M). No explanation was found for this weak effect of HCl concentration (compared to other conventional systems).

It is noteworthy to remind that the experimental conditions have been appropriately selected to really measure the impact of this parameter (i.e., metal excess compared to the concentration of reactive groups).

Sorption Isotherms

Sorption isotherms were compared at two HCl concentrations (i.e., 0.1 M and 1 M) for the three resins prepared by the immobilization of Cyphos IL-101, IL-105 and IL-111, respectively (Fig. 5). Comparing the complete sorption isotherms (i.e., the saturation plateau) allows reaching a more accurate evaluation of the impact of acid concentration (compared to previous section) and IL characteristics.

Table 2 reports the values of model parameters for the different experiments (varying HCl concentration and the type of IL). For Cyphos IL-101 and IL-105 the sorption isotherms were very close as shown by the parameters of the equation (Table 2) and the curves on Fig. 5: the sorption capacity was slightly (about 10%) lower in 1 M HCl solutions (compared to 0.1 M HCl solutions). The differences were less significant (and the sorption capacity even increased when HCl concentration increased) for Cyphos IL-111. The resins have a higher affinity for Cd(II) in 1 M HCl solutions than in 0.1 HCl media. The affinity coefficient was the same (around 2.7 L mg^{-1}) for the three resins in 1 M HCl solutions, while at lower HCl concentration the affinity coefficient decreased by a factor two to three for Cyphos IL-101, IL-105, and IL-111. These variations may be due to different ability for counteranions to be exchanged. At high HCl concentrations these differences are leveled off. The molar ratio, at saturation, between Cd(II) and IL was calculated in order to estimate the

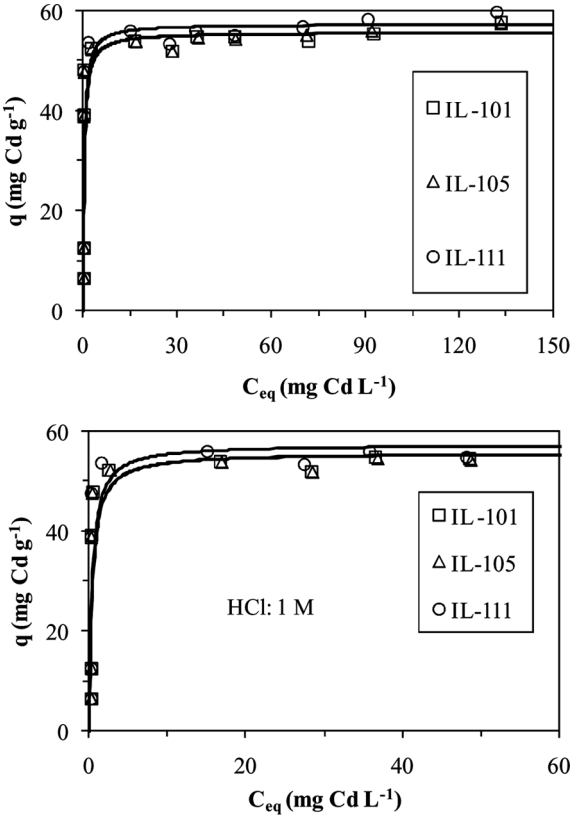

FIG. 5. Cd(II) sorption isotherms in 0.1 M (top) and 1 M (down) HCl solutions using Cyphos IL-101, IL-105 and IL-111 – impregnated resins (lines represent the modeling of experimental data using the Langmuir equation with the parameters reported in Table 3).

stoichiometric ratio. Based on the hypothesis of an interaction between $CdCl_4^{2-}$ and $R_3R'P^+$ (tetraalkyl phosphonium cation) the expected molar ratio should be close to 1:2. Table 2 reports the q_m in mmol Cd per mmol IL: the molar ratio varied between 0.52 and 0.60 for Cyphos IL-101, IL-105, and IL-111 (consistently with expected ratio).

The sorption capacities obtained under acidic conditions are 4 times greater than those obtained by Navarro et al. (19) in the case of Cyanex 921 immobilized on Amberlite XAD-7 (about 15 mg Cd g^{-1}) and about 6 times greater than the values cited by Gonzalez et al. (21) in the case of Cyanex 272 immobilized on Amberlite XAD-2 (about 10 mg Cd g^{-1}). The stoichiometric ratio between the extractant and the metal is more favorable for the IL compared to Cyanex extractants (2:1 to 4:1 depending on the extractant and HCl concentration versus 1:1 for the IL). This probably explains the higher sorption capacity obtained with IL immobilized in alginate capsules. Benamor et al. (18) obtained sorption capacities close to 40 mg Cd g^{-1} using di(2-ethylhexyl) phosphoric acid immobilized on Amberlite XAD-7 (at pH 4). The sorption capacity strongly decreased when decreasing the pH. Wang et al. (57) impregnated 8-hydroxyquinoline-5-sulfonic acid on Lewatit MP 600 and they found sorption capacities close to 52 mg Cd g^{-1} at the highest extractant loading, comparable to those obtained in the present study.

Uptake Kinetics

Table 3 reports the value of D_e for the different sets of experimental data. The intraparticle diffusion coefficient varied between 0.6×10^{-11} and 8×10^{-11} m^2 min^{-1}. This means far below (about 2 orders of magnitude) the molar diffusivity of Cd(II) in water (i.e., 4.3×10^{-9} m^2 min^{-1}). In the case of Amberlite XAD-7 impregnated with di(2-ethylhexyl) phosphoric acid, Benamor et al. (18) concluded that mass transfer was controlled by the resistance to intraparticle diffusion. They found that intraparticle diffusion coefficients varied between 3.0×10^{-10} and 5.5×10^{-10} m^2 min^{-1} (this means between 1 and 2 orders of magnitude greater than the values reached with the present system). For Cd(II) sorption using Cyanex 921 impregnated on Amberlite XAD-7, Navarro et al. (19) obtained intraparticle diffusion coefficient close to 3.2×10^{-10} m^2 min^{-1}. Gonzalez et al. (21) immobilized Cyanex 272 and Cyanex 302 on Amberlite XAD-2 for Cd(II) sorption from acidic solutions. They found that the intraparticle diffusion coefficient varied with the extractant (from 1.6×10^{-10} m^2 min^{-1} for Cyanex 272 to 0.6×10^{-10} m^2 min^{-1} for Cyanex 302). In the case of Cyanex 301-impregnated resins for Cd(II) sorption, Hinojosa Reyes et al. (20) observed

TABLE 2
Sorption isotherms – parameters of the Langmuir equation

	Cyphos IL-101		Cyphos IL-105		Cyphos IL-111	
HCl concentration	0.1 M	1 M	0.1 M	1 M	0.1 M	1 M
q_m (mg Cd g^{-1})	63.4	55.8	62.9	55.7	52.6	57.6
B (L mg^{-1})	0.90	2.63	0.49	2.69	0.33	2.77
q_m (mmol Cd g^{-1})	0.56	0.50	0.56	0.50	0.47	0.51
q_m (mmol Cd/mmol IL)	0.59	0.52	0.60	0.53	0.53	0.58
Estimated variance on q modeling	84	114	138	111	26	118

TABLE 3
Intraparticle diffusion coefficient (D) – impact of experimental parameters

IL Type	C_0 (mg Cd L^{-1})	m/V ($g\,L^{-1}$)	v (rpm)	$D_e \times 10^{11}$ ($m^2\,min^{-1}$)
IL-101	25	0.25	200	2.67
IL-105	25	0.25	200	2.47
IL-111	25	0.25	200	1.14
IL-101	25	0.4	200	0.89
IL-105	25	0.4	200	1.07
IL-111	25	0.4	200	0.63
IL-101	50	0.65	200	1.89
IL-105	50	0.65	200	3.08
IL-111	50	0.65	200	0.93
IL-101	100	0.65	200	5.81
IL-105	100	0.65	200	8.01
IL-111	100	0.65	200	3.24
IL-101	50	0.125	200	4.84
IL-101	50	0.25	200	4.64
IL-101	50	0.4	200	3.87
IL-101	50	0.4	100	3.27
IL-101	50	0.4	500	2.84
IL-101	70	0.4	200	5.38

that the structure properties of the support influence intraparticle diffusion properties: Amberlite XAD-2 exhibited lower intraparticle diffusion coefficient (i.e., $0.5 \times 10^{-10}\,m^2\ min^{-1}$) than Amberlite XAD-7 (i.e., $2.3 \times 10^{-10}\,m^2\ min^{-1}$), probably due to differences in superficial areas (330 and $450\,m^2\ g^{-1}$, respectively). Gallardo et al. (56) tested Zn(II) sorption in HCl solutions using Amberlite XAD-7 impregnated with Cyphos IL-101 they found intraparticle diffusivity coefficients in the range $1–6 \times 10^{-11}\,m^2\ min^{-1}$, depending on experimental conditions.

Cyphos IL-101 immobilized in alginate matrices have been tested for other metal ions, and the intraparticle diffusion coefficients were found in the range $0.7–1.5 \times 10^{-12}\,m^2\ min^{-1}$ for Pd(II) (41), $2–6 \times 10^{-12}\,m^2\ min^{-1}$ for Pt(IV) (42), $1–12 \times 10^{-11}\,m^2\ min^{-1}$ for Hg(II) (43), $1–4 \times 10^{-11}\,m^2\ min^{-1}$ for Au(III) (44), and $0.4–14 \times 10^{-11}\,m^2\ min^{-1}$ for Bi(III) (45). These values are consistent with those found with Cd(II).

Influence of the Structure of the Counteranions of IL

Figure 6 show the kinetic profiles for Cd(II) sorption (at $25\,mg\,L^{-1}$) for different ILs and a sorbent dosage (SD) of $250\,mg\,L^{-1}$(similar trend was obtained with a SD of $400\,mg\,L^{-1}$, not shown). Cyphos IL-101 and IL-105 based resins showed very similar profiles (almost overlapped), a little more favorable than those obtained with

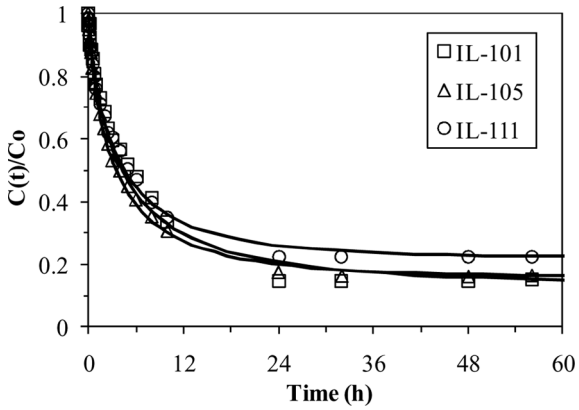

FIG. 6. Influence of IL-structure on Cd(II) uptake kinetics (m/V: $250\,mg\,L^{-1}$; HCl: 1 M; C_0: 25 mg Cd L^{-1}; v: 200 rpm).

Cyphos IL-111 based resin (for which the equilibrium concentration was slightly higher than for other systems). This little difference in the equilibrium performance is probably attributable to the smaller amount of IL in this resin. The intraparticle diffusion equation applied to these systems showed a good correlation between experimental data and simulated profiles, regardless of sorbent dosage and type of IL. The intraparticle diffusion coefficient was of the same order for Cyphos IL-101 and IL-105 materials (the variation in the diffusivity coefficient did not exceed 10%), and slightly higher than the values obtained with Cyphos IL-111 material. The intraparticle diffusion coefficient was halved at the lowest sorbent dosage (i.e., $250\,mg\,L^{-1}$) and decreased by about 40% at higher sorbent dosage (i.e., $400\,mg\,L^{-1}$). This result confirms that the difference in the structure of the IL-impregnated resin impacted the mass transfer properties. However, the variations were not very marked. The comparison is also made complex by slight differences in the IL loading of the different sorbents. Despite the more opened structure that appeared through SEM-EDAX analysis, the synthesis procedure involving the solidification of the IL was not favorable for diffusion properties. However, this hypothesis should be verified by complementary experiments to check that this unfavorable effect cannot be attributed to the exchange properties of the counteranion on Cyphos IL-111.

Increasing the sorbent dosage decreased the intraparticle diffusion coefficient: the value of the intraparticle diffusion coefficient decreased by a factor 2–3 when the sorbent dosage increased from 250 to $400\,mg\,L^{-1}$. Increasing the amount of IL increases the number of reactive groups, while the saturation of the resin decreases. As a consequence the concentration gradient may change and affect mass transfer properties. Nestlé and Kimmich (58) correlated the intraparticle diffusion coefficient to the equilibrium concentration through an equation derived from the Langmuir equation for the sorption of copper with alginate

gel beads (Eq. 10). They used NMR-imaging for the characterization of these systems.

$$D = \frac{(1+bC)^2}{(1+bC)^2 + q_m b} D_0 \quad (10)$$

where D_0 is the diffusion coefficient in the absence of any sorption reaction.

In the present study, the increase of the sorbent dosage results in a decrease of the concentration in the solution (at equilibrium, but probably also during the course of the kinetics), which, in turn, affects the mass transfer according to Nestlé and Kimmich concept.

Figure 7 compares the different ILs based materials with a Cd(II) concentration of 50 mg L^{-1}(similar trend was obtained with an initial metal concentration of 100 mg L^{-1}, not shown). Similar conclusions to those reached with sorbent dosage variation were observed: Cyphos IL-101 and IL-105 based sorbents were very close, regardless of metal concentration. At low Cd(II) concentration, the kinetic profile for IL-111 based resin was very similar to those of other ILs. Increasing metal concentration to 100 mg L^{-1} resulted in a significant diminution in the efficiency of metal sorption (the relative concentration at equilibrium was increased to 0.6–0.7). The comparison of the intraparticle diffusion coefficient showed more marked differences for the three systems: IL-105 > IL-101 ≫IL-111. The intraparticle diffusivity increased by 50% between IL-101 and IL-105 based materials. In this case the two ILs were synthesized according to the same experimental procedure (contrary to IL-111), so these differences are probably related to the exchange of counteranions. However, whatever the system considered, the equilibrium was reached within the first 24 hours (more than 90% of total sorption occurred during the first day of contact).

Since all these ILs were produced by chemical modification of Cyphos IL-101 (precursor for other tested ILs) and because the change in the counteranion did not change a lot the sorption behavior, the study was continued using exclusively Cyphos IL-101 for a more in depth investigation of the effect of sorbent dosage, agitation speed, and metal concentration.

Influence of Agitation Speed on Cd(II) Uptake Kinetic with Cyphos IL-101 Based Resin

The agitation speed may affect the resistance to film diffusion. Figure 8 shows that in the range of agitation speed 100–500 rpm, this parameter did not significantly change the kinetic profiles. The modeling of the curves with the intraparticle diffusion equation was again appropriate for the simulation of the curves and the variation of the intraparticle diffusion coefficient with the agitation speed did not show a clear trend. The intraparticle diffusivity varied between 2.84×10^{-11} and 3.87×10^{-11} m^2 min^{-1} but discontinuously. These results confirm the hypotheses evocated above when testing the shrinking core and the homogeneous diffusion models (with film and intraparticle diffusion resistances to mass transfer, not shown), which suggested that the film diffusion is not the rate controlling step in the process.

Influence of Sorbent Dosage on Cd(II) Uptake Kinetic with Cyphos IL-101 Based Resin

Figure 9 shows that whatever the sorbent dosage (m/V) the equilibrium was reached within the first 24 hours of contact. The kinetic profiles were well fitted by the intraparticle diffusion equation (Crank's equation), as shown by the perfect superimposition of experimental data and modeled curves. Increasing sorbent dosage obviously decreased the equilibrium relative concentration (C/C_0), and the intraparticle diffusion coefficient. Taking into account the equilibrium concentration for the different series of experiments it was possible to correlate the diffusion

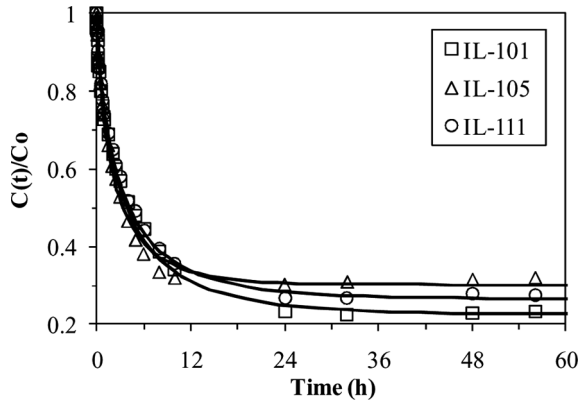

FIG. 7. Influence of IL-structure on Cd(II) uptake kinetics (C_0: 50 mg Cd L^{-1}; HCl: 1 M; m/V: 650 mg L^{-1}; v: 200 rpm).

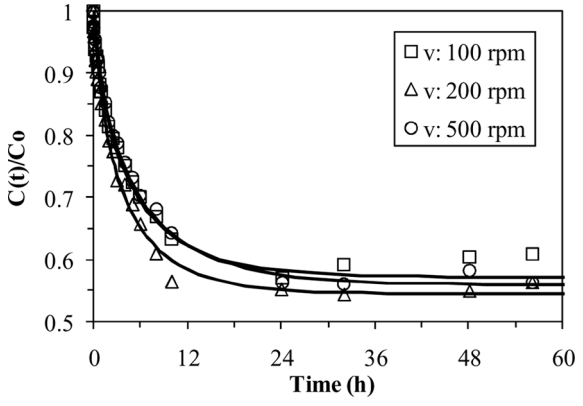

FIG. 8. Influence of agitation speed on Cd(II) uptake kinetics using Cyphos IL-101 – immobilized resin (HCl: 1 M; C_0: 50 mg L^{-1}; m/V: 400 mg L^{-1}).

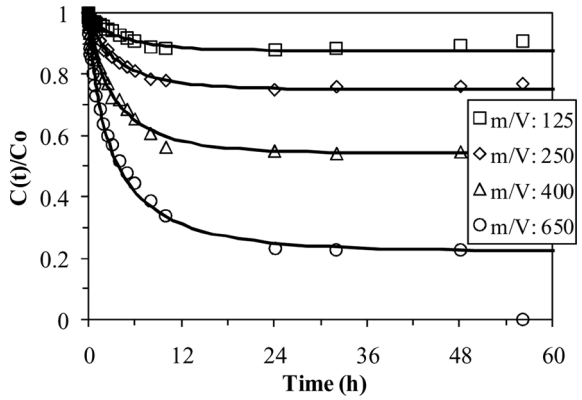

FIG. 9. Influence of m/V on Cd(II) uptake kinetics using Cyphos IL-101 – immobilized resin (HCl: 1 M; C_0: 50 mg L^{-1}; v: 200 rpm).

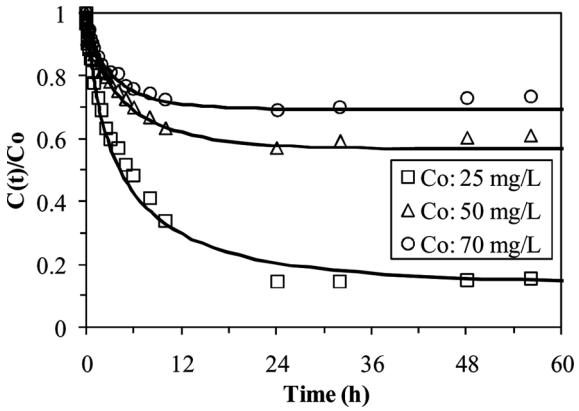

FIG. 11. Influence of metal concentration on Cd(II) uptake kinetics using Cyphos IL-101 – immobilized resin (HCl: 1 M; m/V: 400 mg L^{-1}; v: 200 rpm).

coefficient according the equation (Langmuir-type; correlation coefficient $R^2 = 0.998$) (Fig. 10):

$$D = \frac{D_m \beta C_{eq}}{1 + \beta C_{eq}} = \frac{9.1 \times 10^{-11} \times 0.025 \times C_{eq}}{1 + 0.025 \times C_{eq}} \qquad (11)$$

Influence of Metal Concentration on Cd(II) Uptake Kinetic with Cyphos IL-101 Based Resin

Figure 11 shows the modeling of kinetic profiles with the intraparticle diffusion equation for varying metal concentration. The intraparticle diffusion model fitted well experimental data and the intraparticle diffusion coefficient increased with metal concentration. (from 0.89×10^{-11} to 5.38×10^{-11} m^2 min^{-1} when increasing metal concentration from 25 to 70 mg L^{-1}). This is related to an increase in the concentration gradient between the external concentration and the internal concentration that improves mass transfer when increasing metal concentration in the solution. Additionally, according to the concept developed by Nestlé and Kimmich, the intraparticle diffusion increases with solute concentration in the solutions. This is consistent with the present results.

All the results obtained with Cyphos IL-101 impregnated resins (for which we had a greater number of experiments) were collected and the equilibrium concentrations were used for calculating the theoretical intraparticle diffusion coefficients with Eq. (11). The calculated values were compared with the results of the model (Fig. 12). The comparison shows that Eq. (11) accurately predicted the intraparticle diffusivity coefficient as a function of equilibrium concentration using the Langmuir-type equation. This empirical equation fitted much better experimental data than the values obtained from the mechanistic equation proposed by Nestle and Kimmich (i.e., Eq. (10)), the

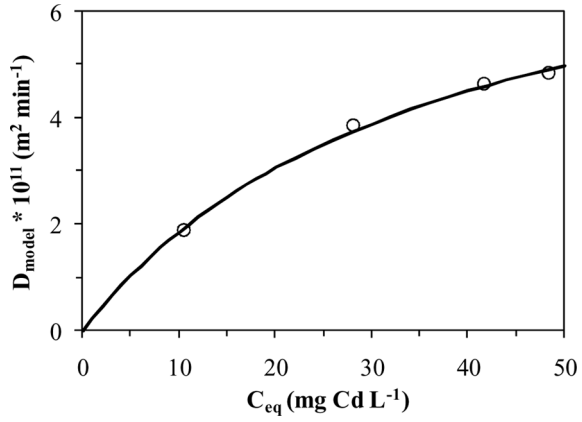

FIG. 10. Variation of the intraparticle diffusion coefficient with equilibrium concentration (derived from Figure 9) and modeling of the curve with Eq. (11).

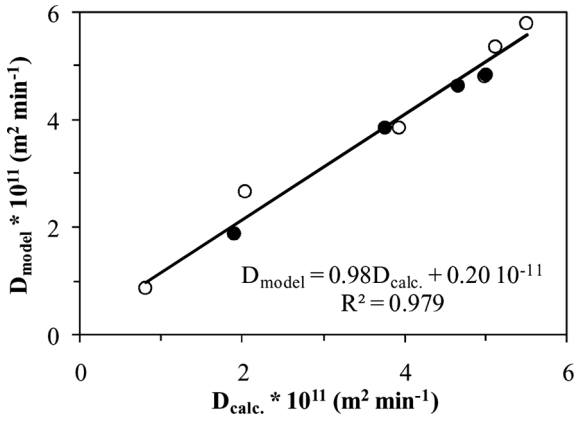

FIG. 12. Simulation of the intraparticle diffusion coefficient with the Langmuir-type equation (Eq. 11) (close symbols represent data that served for determining the parameters of the equation; open symbols are testing data; continuous line shows the linear regression obtained on the totality of the data).

experimental data, plotted versus calculated data, were not linearly distributed, contrary to the empirical equation (i.e., Eq. (11)) (Not shown).

Improvement of Diffusion Properties

The comparison of intraparticle diffusion coefficients for Cyphos IL-101 immobilized on alginate capsules with those obtained using conventional resins impregnated with extractants (see above) and the diagnostic of the resistance to intraparticle diffusion as the limiting step for uptake kinetics point out the need for improving the mass transfer properties of these materials. Previous studies have indicated that the drying of the resins at the end of the process caused a decrease of the diffusion properties (42,43). Controlling the drying step is not feasible using a drying under supercritical CO_2 conditions (59), since the solvent exchange with ethanol could provoke the loss of the IL. Alginate sponges with IL immobilized in the polymer matrix have been prepared to synthesize highly porous monoliths using a procedure derived from Madihally and Matthew (60). Figure 13 shows an example of monolith produced according to this procedure (SEM analysis). These materials are currently under investigation.

Cadmium Desorption and Resin Recycling

Metal desorption from loaded resin, and resin re-use are key-criterions in the evaluation of the sorption performance of these materials. Hinojosa Reyes et al. (20) used several acidic, neutral, and complexing agents for Cd(II) stripping from Cyanex 301-impregnated Amberlite XAD-2 resins. They found that HCl solutions gave a higher desorption yield in a single step. The encapsulating material (alginate) used for the immobilization of ILs being unstable in alkaline and even neutral solutions, desorption should proceed in acidic medium. Several acidic solutions have been tested (i.e., HCl, HNO_3, and H_2SO_4) at different concentrations (i.e., 0.1 and 0.5 M). Hydrochloric acid was not efficient at all for Cd(II) stripping with both 0.1 and 0.5 M concentrations: desorption yield did not exceed 2%. This is probably due to the strong affinity of Cd(II) for chloride anions and to the formation of chloro-anionic complexes, which are stably bound to phosphonium cation. With sulfuric acid, desorption reached values close to 90%: the efficiency decreased when increasing the concentration of the acid (from 93% to 88%). Regel Rosocka (27) also used sulfuric acid for Zn(II) stripping from loaded Cyphos IL-101/toluene phase. They obtained a high efficiency for metal extraction and metal stripping for 4 cycles. However, in the present case, the highest desorption was reached with nitric acid with efficiencies greater than 96%; in this case the efficiency slightly increased with acid concentration (from 96% to 98% increasing HNO_3 concentration from 0.1 M to 0.5 M). Since sulfate and nitrate anions do not form stable anionic complexes with cadmium this may explain that the corresponding acids could remove the metal from loaded resins.

Table 4 reports the results obtained along three cycles for Cd(II) recovery from 1 M HCl solutions with Cyphos IL-101 immobilized capsules for the different sets of eluents (nitric and sulfuric acids at concentrations 0.1 and 0.5 M). Sorption efficiency (and relative sorption capacity) did not significantly vary along the three cycles: the

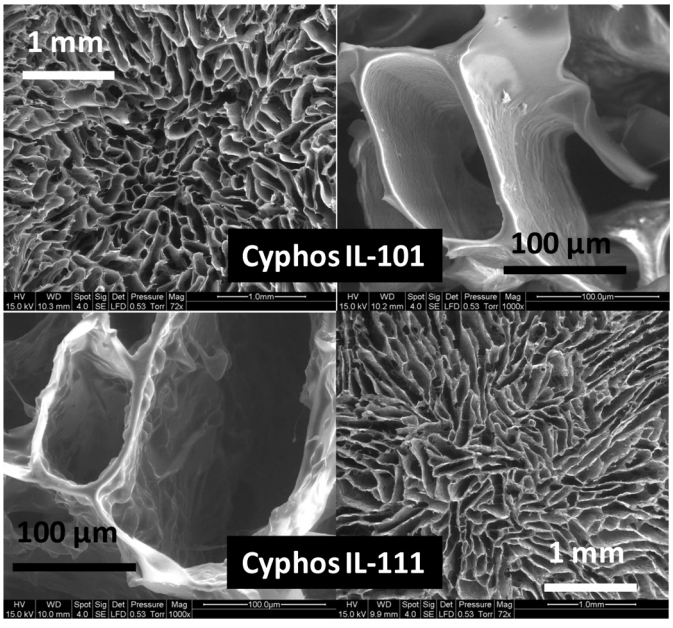

FIG. 13. Examples of monolith produced for the immobilization of Cyphos IL-101 and Cyphos IL-111 in highly porous alginate matrix (SEM photographs).

TABLE 4
Resin reuse

Eluent	Cycle number	Adsorption Efficiency (%)	Adsorption Capacity (mg Cd g^{-1})	Desorption efficiency (%)
	1	69	57.5	96
HNO_3	2	63	52.4	>99
0.1 M	3	63	52.0	94
	1	66	55.7	98
HNO_3	2	64	53.0	98
0.5 M	3	64	53.1	90
	1	69	57.3	93
H_2SO_4	2	64	52.8	>99
0.1 M	3	62	51.3	87
	1	67	56.0	88
H_2SO_4	2	64	52.6	91
0.5 M	3	64	52.5	84

decrease did not exceed 10%. On the other hand, the desorption yield remained almost constant for the first two cycles and slightly decreased at the third cycle. However, with nitric acid, regardless of acid concentration, the sorption levels and the desorption efficiencies were maintained at high levels: around 65% of sorption under selected experimental conditions and about 96% of desorption efficiency as an average value for the three cycles.

These results show that nitric acid at concentrations in the range 0.1–0.5 M can be used for metal desorption from Cd(II)-loaded Cyphos IL-101 immobilized capsules and for their recycling, for at least 3 cycles.

CONCLUSION

Tetraalkyl phosphonium ILs (Cyphos "family") have been tested under comparable experimental conditions for the sorption of Cd(II) in hydrochloric acid solutions. The counterpart of the phosphonium cation did not greatly influence sorption properties, except in the case of Cyphos IL-109 (bistriflamide substitute). Its sorption properties were strongly depleted (almost no sorption of Cd(II)) probably due to the impact of hydrophobic effect or poor exchangeability of amide compound). The physical state of Cyphos IL-111 (tetrafluoroborate), solid at room temperature, affected the internal structure of the capsules (large vesicles seen on SEM analysis of particle cross-section) but weakly influenced sorption isotherms and uptake kinetics. The mechanism involved in Cd(II) binding consists in an ion exchange mechanism between cadmium chloroanionic species ($CdCl_4^{2-}$) and the counteranion of the IL. At saturation of the resin the stoichiometric molar ratio Cd(II)/IL varied between 0.52 and 0.60; the theoretical stoichiometric ratio, based on fully accessible reactive groups is 0.5. The resins have a strong affinity for Cd(II) as shown by the sharp initial slope of the isotherm curves. The kinetics were governed by the resistance to intraparticle diffusion: kinetic curves were perfectly fitted by the model. The poor effect of agitation speed confirmed the limited impact of the resistance to film diffusion on the overall kinetics. The intraparticle diffusion coefficients were correlated with the equilibrium concentration (according to a Langmuir-type equation). Metal desorption can be operated using nitric acid (at a concentration between 0.1 and 0.5 M), and sorption properties were maintained for at least 3 sorption/desorption cycles.

ACKNOWLEDGEMENTS

C.J., T.V., and E.G. acknowledge the financial funding from Carnot Institute for the research program "Encapsulation de liquides ioniques" (07AS 11 LGEI1); A.F.P. acknowledges the grant from Erasmus European Program for her training period at Ecole des Mines d'Alès. Authors thank Cytec (Canada) for supplying the IL and Jean-Marie Taulemesse (Ecole des Mines d'Alès, CMGD) for SEM-EDAX analysis.

REFERENCES

1. Rudnik, E.; Nikiel, M. (2007) Hydrometallurgical recovery of cadmium and nickel from spent Ni-Cd batteries. *Hydrometallurgy*, 89 (1–2): 61.
2. Nogueira, C.A.; Margarido, F. (2004) Leaching behaviour of electrode materials of spent nickel-cadmium batteries in sulphuric acid media. *Hydrometallurgy*, 72 (1–2): 111.
3. Nogueira, C.A.; Delmas, F. (1999) New flowsheet for the recovery of cadmium, cobalt and nickel from spent Ni-Cd batteries by solvent extraction. *Hydrometallurgy*, 52 (3): 267.
4. Bartolozzi, M.; Braccini, G.; Bonvini, S.; Marconi, P.F. (1995) Hydrometallurgical recovery process for nickel-cadmium spent batteries. *Journal of Power Sources*, 55 (2): 247.
5. Vassura, I.; Morselli, L.; Bernardi, E.; Passarini, F. (2009) Chemical characterisation of spent rechargeable batteries. *Waste Management*, 29 (8): 2332.
6. Nogueira, C.A.; Margarido, F. (2007) Chemical and physical characterization of electrode materials of spent sealed Ni-Cd batteries. *Waste Management*, 27 (11): 1570.
7. Brooks, C.S. (1991) *Metal Recovery from Industrial Wastes*; Lewis Publishers: Chelsea, MI.
8. Reddy, B.R.; Priya, D.N.; Park, K.H. (2006) Separation and recovery of cadmium(II), cobalt(II) and nickel(II) from sulphate leach liquors of spent Ni-Cd batteries using phosphorus based extractants. *Sep. Purif. Technol.*, 50 (2): 161.
9. Reddy, B.R.; Priya, D.N. (2006) Chloride leaching and solvent extraction of cadmium, cobalt and nickel from spent nickel-cadmium, batteries using Cyanex 923 and 272. *Journal of Power Sources*, 161 (2): 1428.
10. Reddy, B.R.; Neela Priya, D.; Venkateswara Rao, S.; Radhika, P. (2005) Solvent extraction and separation of Cd(II), Ni(II) and Co(II) from chloride leach liquors of spent Ni-Cd batteries using commercial organo-phosphorus extractants. *Hydrometallurgy*, 77 (3–4): 253.
11. Rickelton, W.A. (1999) The extraction of cadmium from a mixture of phosphoric and hydrochloric acids. *Solvent Extr. Ion Exch.*, 17 (6): 1507.
12. Nayak, A.K.; Mishra, P.K.; Panda, C.R.; Chakravorrty, V. (1995) Solvent extraction of zinc(II) and cadmium(II) by Cyanex 272, 301 and 302. *Indian J. Chem. Technol.*, 2 (2): 111.
13. Almela, A.; Elizalde, M.P. (1995) Solvent extraction of cadmium(II) from acidic media by Cyanex 302. *Hydrometallurgy*, 37 (1): 47.
14. Wang, F.; Wang, L.-J.; Li, J.-S.; Sun, X.-Y.; Han, W.-Q. (2009) Adsorption behavior and mechanism of cadmium on strong-acid cation exchange resin. *Trans. Nonferrous Met. Soc. China*, 19 (3): 740.
15. Bedoui, K.; Bekri-Abbes, I.; Srasra, E. (2008) Removal of cadmium (II) from aqueous solution using pure smectite and Lewatite S 100: the effect of time and metal concentration. *Desalination*, 223 (1–3): 269.
16. Senkal, B.F.; Ince, M.; Yavuz, E.; Yaman, M. (2007) The synthesis of new polymeric sorbent and its application in preconcentration of cadmium and lead in water samples. *Talanta*, 72 (3): 962.
17. Malla, M.E.; Alvarez, M.B.; Batistoni, D.A. (2002) Evaluation of sorption and desorption characteristics of cadmium, lead and zinc on Amberlite IRC-718 iminodiacetate chelating ion exchanger. *Talanta*, 57 (2): 277.
18. Benamor, M.; Bouariche, Z.; Belaid, T.; Draa, M.T. (2008) Kinetic studies on cadmium ions by Amberlite XAD7 impregnated resins containing di(2-ethylhexyl) phosphoric acid as extractant. *Sep. Purif. Technol.*, 59 (1): 74.

19. Navarro, R.; Saucedo, I.; Nunez, A.; Avila, M.; Guibal, E. (2008) Cadmium extraction from hydrochloric acid solutions using Amberlite XAD-7 impregnated with Cyanex 921 (tri-octyl phosphine oxide). *React. Funct. Polym.*, 68 (2): 557.
20. Hinojosa Reyes, L.; Saucedo Medina, T.I.; Navarro Mendoza, R.; Revilla Vasquez, J.; Avila Rodriguez, M.; Guibal, E. (2001) Extraction of cadmium from phosphoric acid using resins impregnated with organophosphorus extractants. *Ind. Eng. Chem. Res.*, 40 (5): 1422.
21. Gonzalez, M.P.; Saucedo, I.; Navarro, R.; Avila, M.; Guibal, E. (2001) Selective separation of Fe(III), Cd(II), and Ni(II) from dilute solutions using solvent-impregnated resins. *Ind. Eng. Chem. Res.*, 40 (25): 6004.
22. Kubota, F.; Koyanagi, Y.; Nakashima, K.; Shimojo, K.; Kamiya, N.; Goto, M. (2008) Extraction of lanthanide ions with an organophosphorous extractant into ionic liquids. *Solv. Extr. Res. Dev.*, 15: 81.
23. Visser, A.E.; Swatloski, R.P.; Reichert, W.M.; Mayton, R.; Sheff, S.; Wierzbicki, A.; Davis, J.H.; Rogers, R.D. (2002) Task-specific ionic liquids incorporating novel cations for the coordination and extraction of Hg^{2+} and Cd^{2+}: Synthesis, characterization, and extraction studies. *Environ. Sci. Technol.*, 36 (11): 2523.
24. Dietz, M.L. (2006) Ionic liquids as extraction solvents: Where do we stand? *Sep. Sci. Technol.*, 41 (10): 2047.
25. Nakashima, K.; Kubota, F.; Maruyama, T.; Goto, M. (2005) Feasibility of ionic liquids as alternative separation media for industrial solvent extraction processes. *Ind. Eng. Chem. Res.*, 44 (12): 4368.
26. Ciezynska, A.; Regel-Rosocka, M.; Wisniewski, M. (2007) Extraction of palladium(II) ions from chloride solutions with phosphonium ionic liquid Cyphos IL101. *Pol. J. Chem. Technol.*, 9 (2): 99.
27. Regel-Rosocka, M. (2009) Extractive removal of zinc(II) from chloride liquors with phosphonium ionic liquids/toluene mixtures as novel extractants. *Sep. Purif. Technol.*, 66 (1): 19.
28. Marták, J.; Schlosser, Š. (2007) Extraction of lactic acid by phosphonium ionic liquids. *Sep. Purif. Technol.*, 57 (3): 483.
29. Marták, J.; Schlosser, Š.; Vlčková, S. (2008) Pertraction of lactic acid through supported liquid membranes containing phosphonium ionic liquid. *J. Membr. Sci.*, 318 (1–2): 298.
30. van den Berg, C.; Wierckx, N.; Vente, J.; Bussmann, P.; de Bont, J.; van der Wielen, L. (2008) Solvent-impregnated resins as an in situ product recovery tool for phenol recovery from *Pseudomonas putida* S12TPL fermentations. *Biotechnol. Bioeng.*, 100 (3): 466.
31. Sun, X.Q.; Peng, B.; Ji, Y.; Chen, J.; Li, D.Q. (2008) The solid-liquid extraction of yttrium from rare earths by solvent (ionic liquid) impregnated resin coupled with complexing method. *Sep. Purif. Technol.*, 63 (1): 61.
32. Myasoedova, G.V.; Molochnikova, N.P.; Mokhodoeva, O.B.; Myasoedov, B.F. (2008) Application of ionic liquids for solid-phase extraction of trace elements. *Anal. Sci.*, 24 (10): 1351.
33. van den Berg, C.; Roelands, M.; Bussmann, P.; Goetheer, E.; Verdoes, D.; van der Wielen, L. (2008) Extractant selection strategy for solvent-impregnated resins in fermentations. *Ind. Eng. Chem. Res.*, 47 (24): 10071.
34. Guibal, E.; Vincent, T.; Jouannin, C. (2009) Immobilization of extractants in biopolymer capsules for the synthesis of new resins: a focus on the encapsulation of tetraalkyl phosphonium ionic liquids. *J. Mater. Chem.*, DOI:10.139/b911318e
35. Fournel, L.; Navarro, R.; Saucedo, I.; Guibal, E. (2002) Cadmium extraction with Cyanex 302 impregnated chitosan beads. In: *International Biohydrometallurgy Symposium, IBS'01*, Ouro Preto, M.G.; (Brazil), Ciminelli, V.S.T.; Garcia, O.J., eds.; Elsevier Science B.V.: Amsterdam, Vol. 2, 109–118.
36. Mimura, H.; Hoshi, H.; Akiba, K.; Onodera, Y. (2001) Separation of americium from europium by biopolymer microcapsules enclosing Cyanex 301 extractant. *J. Radioanal. Nucl. Chem.*, 247 (2): 375.
37. Mimura, H.; Ohta, H.; Akiba, K.; Wakui, Y.; Onodera, Y. (2002) Uptake and recovery of platinum group metals ions by alginate microcapsules immobilizing Cyanex 302 emulsions. *J. Nucl. Sci. Technol.*, 39 (9): 1008.
38. Mimura, H.; Ohta, H.; Hoshi, H.; Akiba, K.; Onodera, Y. (2001) Uptake properties of palladium for biopolymer microcapsules enclosing Cyanex 302 extractant. *Sep. Sci. Technol.*, 36 (1): 31.
39. Ngomsik, A.-F.; Bee, A.; Siaugue, J.-M.; Talbot, D.; Cabuil, V.; Cote, G. (2009) Co(II) removal by magnetic alginate beads containing Cyanex 272. *J. Hazard. Mater.*, 166 (2–3): 1043.
40. Outokesh, M.; Mimura, H.; Niibori, Y.; Tanaka, K. (2006) Equilibrium and kinetics of silver uptake by multinuclear alginate microcapsules comprising an ion exchanger matrix and Cyanex 302 ogranophosphinic acid extractant. *Ind. Eng. Chem. Res.*, 45 (10): 3633.
41. Vincent, T.; Parodi, A.; Guibal, E. (2008) Immobilization of Cyphos IL-101 in biopolymer capsules for the synthesis of Pd sorbents. *React. Funct. Polym.*, 68 (7): 1159.
42. Vincent, T.; Parodi, A.; Guibal, E. (2008) Pt recovery using Cyphos IL-101 immobilized in biopolymer capsules. *Sep. Purif. Technol.*, 62 (2): 470.
43. Guibal, E.; Campos, K.; Bunio, P.; Vincent, T.; Trochimczuk, A. (2008) Cyphos IL 101 (tetradecyl(trihexyl)phosphonium chloride) immobilized in biopolymer capsules for Hg(II) recovery from HCl solutions. *Sep. Sci. Technol.*, 43 (9): 2406.
44. Campos, K.; Vincent, T.; Bunio, P.; Trochimczuk, A.; Guibal, E. (2008) Gold recovery from HCl solutions using Cyphos IL-101 (a quaternary phosphonium ionic liquid) immobilized in biopolymer capsules. *Solvent Extr. Ion Exch.*, 26 (5): 570.
45. Campos, K.; Domingo, R.; Vincent, T.; Ruiz, M.; Sastre, A.M.; Guibal, E. (2008) Bismuth recovery from acidic solutions using Cyphos IL-101 immobilized in a composite biopolymer matrix. *Water Res.*, 42 (14): 4019.
46. Papageorgiou, S.K.; Kouvelos, E.P.; Katsaros, F.K. Calcium alginate beads from Laminaria digitata for the removal of Cu^{+2} and Cd^{+2} from dilute aqueous metal solutions, in 2nd International Conference on Water Science and Technology – Integrated Management of Water Resources, Athens, GREECE, Nov 23–26, Eds., Vol. 293–306.
47. Davis, T.A.; Ramirez, M.; Mucci, A.; Larsen, B. (2004) Extraction, isolation and cadmium binding of alginate from Sargassum spp. *J. Appl. Phycol.*, 16 (4): 275.
48. Davis, T.A.; Llanes, F.; Volesky, B.; Mucci, A. (2003) Metal selectivity of Sargassum spp. and their alginates in relation to their alpha-L-guluronic acid content and conformation. *Environ. Sci. Technol.*, 37 (2): 261.
49. Guibal, E. (2004) Interactions of metal ions with chitosan-based sorbents: a review. *Sep. Purif. Technol.*, 38 (1): 43.
50. Streat, M. (1984) Kinetics of slow diffusing species in ion exchangers. *React. Polym.*, 2 (1–2): 79.
51. Helfferich, F. (1995) *Ion Exchange*, 2nd Ed.; Dover Publications, Inc.: Mineola, N.Y.
52. Juang, R.-S.; Ju, C.-Y. (1998) Kinetics of sorption of Cu(II)-ethylenediaminetetraacetic acid chelated anions on cross-linked, polyaminated chitosan beads. *Ind. Eng. Chem. Res.*, 37 (8): 3463.
53. Juang, R.-S.; Lin, H.-C. (1995) Metal sorption with extractant-impregnated macroporous resins. 1. Particle diffusion kinetics. *J. Chem. Technol. Biotechnol.*, 62 (2): 132.
54. Juang, R.-S.; Lin, H.-C. (1995) Metal sorption with extractant-impregnated macroporous resins. 2. Chemical reaction and particle diffusion kinetics. *J. Chem. Technol. Biotechnol.*, 62 (2): 141.
55. Vincent, T.; Guibal, E.; Chiarizia, R. (2007) Palladium recovery by reactive precipitation using a Cyanex 301-based stable emulsion. *Sep. Sci. Technol.*, 42 (16): 3517.

56. Gallardo, V.; Navarro, R.; Saucedo, I.; Avila, M.; Guibal, E. (2007) Zinc(II) extraction from hydrochloric acid solutions using amberlite XAD-7 impregnated with Cyphos IL 101 (tetradecyl(trihexyl)phosphonium chloride). *Sep. Sci. Technol.*, 43 (9–10): 2434.
57. Wang, Y.; Wang, C.Y.; Warshawsky, A.; Berkowitz, B. (2003) 8-hydroxyquinoline-5-sulfonic acid (HQS) impregnated on Lewatit MP 600 for cadmium complexation: Implication of solvent impregnated resins for water remediation. *Sep. Sci. Technol.*, 38 (1): 149.
58. Nestle, N.; Kimmich, R. (1996) Concentration-dependent diffusion coefficients and sorption isotherms. Application to ion exchange processes as an example. *J. Phys. Chem.*, 100 (30): 12569.
59. Robitzer, M.; David, L.; Rochas, C.; Di Renzo, F.; Quignard, F. (2008) Nanostructure of calcium alginate aerogels obtained from multistep solvent exchange route. *Langmuir*, 24 (21): 12547.
60. Madihally, S.V.; Matthew, H.W.T. (1999) Porous chitosan scaffolds for tissue engineering. *Biomaterials*, 20 (12): 1133.